EUROPHYSICS LETTERS 15 January 2005

Europhys. Lett., **69** (2), pp. 170–176 (2005)
DOI: 10.1209/epl/i2004-10327-x

Frequency locking in extended systems: The impact of a Turing mode

A. Yochelis[1], C. Elphick[2], A. Hagberg[3] and E. Meron[4,5]

[1] *Department of Chemical Engineering, Technion, Israel Institute of Technology 32000 Haifa, Israel*
[2] *Centro de Fisica No Lineal y Sistemas Complejos de Santiago Casilla 17122, Santiago, Chile*
[3] *Mathematical Modeling and Analysis, Theoretical Division Los Alamos National Laboratory - Los Alamos, NM 87545, USA*
[4] *Department of Physics, Ben Gurion University - Beer Sheva 84105, Israel*
[5] *Department of Solar Energy and Environmental Physics, BIDR Ben Gurion University - Sede Boker Campus 84990, Israel*

received 28 June 2004; accepted in final form 8 November 2004
published online 17 December 2004

PACS. 05.45.Xt – Synchronization; coupled oscillators.
PACS. 47.20.Ky – Nonlinearity (including bifurcation theory).
PACS. 47.54.+r – Pattern selection; pattern formation.

Abstract. – A Turing mode in an extended periodically forced oscillatory system can change the classical resonance boundaries of a single forced oscillator. Using the normal form equation for forced oscillations, we identify a Hopf-Turing bifurcation point around which we perform a weak nonlinear analysis. We show that resonant standing waves can exist outside the 2 : 1 resonance region of uniform oscillations, and non-resonant mixed-mode oscillations may prevail inside the resonance region.

An oscillator, periodically forced in time, can adjust its oscillation frequency to make it a rational fraction of the forcing frequency [1]. At very low forcing amplitudes, the forced oscillator exhibits quasi-periodic oscillations consisting of the forcing frequency and the frequency of the unforced oscillator. Frequency adjustment, or frequency locking, occurs when the forcing amplitude exceeds a threshold value that depends on the forcing frequency. In the parameter plane spanned by the forcing amplitude and forcing frequency, these thresholds form tongue-shaped regions, the so-called Arnol'd tongues. Each tongue corresponds to a different rational relation between the forcing frequency and the oscillation frequency and designates a domain of frequency locking, or resonance, where the oscillation is strictly periodic [1].

Spatially extended systems often show synchronous oscillations where all spatial elements share the same frequency and phase of oscillations. These oscillations usually arise through a Hopf bifurcation where a spatially uniform Hopf mode grows from an unstable stationary state. When the oscillations are periodically forced they may exhibit frequency locking like

single oscillators. Spatial coupling in oscillating media, however, may lead to finite-wave-number, or Turing, instabilities [2] which break the translational phase symmetry; different spatial regions may not share the same oscillation phase. Frequency-locking phenomena in spatially extended systems have been studied in various contexts, including autocatalytic surface reactions [3], charge-density-wave conductors [4], cardiac activity [5], and chemical reactions [6]. The possible effects of spatial instabilities on frequency locking, however, have not been considered in these studies [7].

In this letter we focus on the 2 : 1 resonance, where the system frequency locks to the forcing at exactly half the forcing frequency. We show that the coupling of a Turing mode [8,9] to the Hopf mode can *extend* or, even more surprisingly, *reduce* the domain of the 2 : 1 resonance. Our analysis is based on the normal form equation for forced oscillations near the Hopf bifurcation, the forced complex Ginzburg-Landau (CGL) equation. The effect of spatial coupling on frequency locking in extended oscillatory systems has already been pointed out by Park [10], but has not been related to a Turing instability.

Consider an extended system with a Hopf bifurcation to uniform oscillations at a frequency Ω, and that is periodically forced at a frequency $\omega_{\rm f} \approx 2\Omega$. Near the Hopf bifurcation a typical dynamical variable of the system can be written as

$$u = u_0 + \left[A e^{i\omega_{\rm f} t/2} + \text{c.c.}\right] + \cdots , \tag{1}$$

where u_0 is the value of u at the rest state, A is a complex amplitude, c.c. stands for the complex conjugate, and the ellipses denote higher-order terms. The amplitude of oscillation A may vary slowly in space and time and for weak forcing is described by the forced CGL equation [11]

$$\partial_t A = (\mu + i\nu)A + (1 + i\alpha)\nabla^2 A - (1 + i\beta)|A|^2 A + \gamma A^* . \tag{2}$$

In this equation, μ represents the distance from the Hopf bifurcation, $\nu = \Omega - \omega_{\rm f}/2$ is the detuning, α represents dispersion, β represents a nonlinear frequency correction, γ is the forcing amplitude. In this study all the parameters except ν are assumed to be non-negative. The term A^* is the complex conjugate of A and describes the effect of the weak periodic forcing [11]. Throughout this paper we will mostly be concerned with eq. (2) for the *amplitude* of oscillations. The oscillating system represented by eq. (1) will be referred to as the "original system".

According to eq. (1), stationary solutions of eq. (2) describe frequency-locked oscillations of the original system (for then u oscillates at exactly half the forcing frequency, despite the fact that the unforced system may oscillate at nearly that frequency). To find the frequency-locking boundary of a single oscillator, we look for stationary *spatially uniform* solutions of eq. (2). Four such solutions appear in a pair of saddle-node bifurcations at $\gamma = \gamma_{\rm b} = |\nu - \mu\beta|/\sqrt{1+\beta^2}$ [12,13], two of which, $A_\pm = \mathcal{R}\exp[i\phi_\pm]$, are stable to uniform perturbations, where

$$\phi_- = \frac{1}{2}\arcsin\frac{\nu - \beta\mathcal{R}^2}{\gamma}, \qquad \phi_+ = \phi_- + \pi, \tag{3a}$$

$$\mathcal{R}^2 = \frac{\mu + \nu\beta + \sqrt{(1+\beta^2)\,\gamma^2 - (\nu - \mu\beta)^2}}{1+\beta^2} . \tag{3b}$$

The solutions describe frequency-locked uniform oscillations with phases differing by π. The existence range of these solutions, $\gamma \geq \gamma_{\rm b}$, forms a V-shaped region in the ν-γ parameter plane, as fig. 1 shows. We call these solutions "phase states", and refer to the V-shaped region as the "2 : 1 resonance tongue" [14, 15].

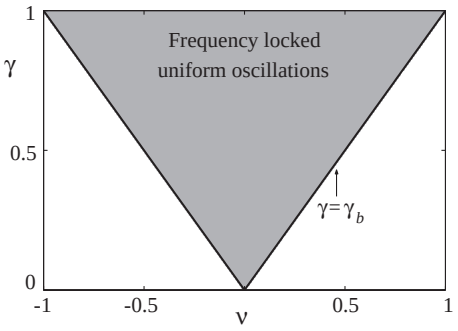

Fig. 1

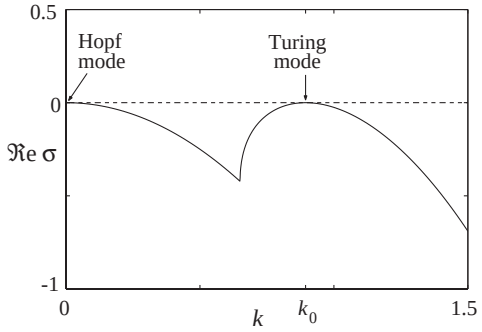

Fig. 2

Fig. 1 – The resonance tongue of spatially uniform solutions of eq. (2) in the ν-γ plane (shaded region). Inside the tongue the original system responds at exactly half of the forcing frequency. Parameters: $\mu = 0.1$, $\beta = 0$, $\alpha = 0.5$.

Fig. 2 – The growth rate (real part of σ) of perturbations from the $A = 0$ state at the codimension-two point, $\mu = 0$, $\gamma = \gamma_c$. Two modes become marginal at this point, a Hopf zero-k mode and a Turing finite-k mode. Parameters: $\mu = 0$, $\nu = 2.0$, $\alpha = 0.5$, $\gamma = \gamma_c \approx 1.8$.

We now study translational symmetry breaking in the extended system described by eq. (2) by considering the stability of the two phase states, ϕ_+ and ϕ_- [16], and the rest state, $A = 0$ [14], to non-uniform perturbations. The linear stability analysis of the phase states indicates a narrow range near the $2:1$ resonance boundary where a finite-wave-number instability leads to stationary patterns [15]. These patterns, however, represent resonant oscillations of the original system and do not affect the $2:1$ resonance boundaries.

In the case of a single forced oscillator, the rest state, $A = 0$, goes through a Hopf bifurcation at $\mu = 0$. The rest state of the extended system, however, may go through a finite-wave-number, or Turing, instability as well. The dispersion relation associated with the rest state is given by [14]

$$\sigma = \mu - k^2 + \sqrt{\gamma^2 - (\nu - \alpha k^2)^2}. \tag{4}$$

An examination of this relation reveals a codimension-two point,

$$\mu = 0, \qquad \gamma = \gamma_c = \nu/\sqrt{1+\alpha^2}, \tag{5}$$

where the Hopf bifurcation to uniform oscillations coincides with a Turing instability [14], as fig. 2 shows. The Hopf frequency and the Turing wave number are given by $\omega_0 = \nu\alpha/\rho$ and $k_0^2 = \nu\alpha/\rho^2$, respectively, where $\rho = \sqrt{1+\alpha^2}$.

To study the system in the vicinity of the codimension-two point, where $|\gamma - \gamma_c| \sim \mu \ll \gamma_c$, we can expand solutions of eq. (2) as

$$\begin{pmatrix} \mathrm{Re}\, A \\ \mathrm{Im}\, A \end{pmatrix} = \left\{ \boldsymbol{e}_0 B_0 e^{i\omega_0 t} + \boldsymbol{e}_k B_k e^{ik_0 x} + \text{c.c.} \right\} + \cdots . \tag{6}$$

The complex amplitudes $B_0(\mu t)$ and $B_k(\mu t)$ in eq. (6) are of order $\sqrt{\mu}$, and describe slow uniform modulations of the (relatively) fast oscillations associated with the Hopf mode and of the fast spatial variations associated with the Turing mode. The more general case, where the amplitudes are also modulated in space, will be discussed elsewhere [17]. The eigenvectors $\boldsymbol{e}_0$ and $\boldsymbol{e}_k$ correspond to the Hopf and the Turing eigenvalues, respectively.

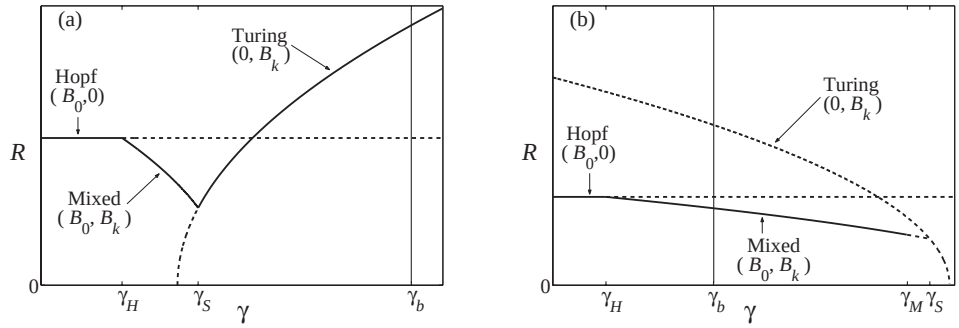

Fig. 3 – Bifurcation diagrams for uniform solutions of eq. (7) showing the existence and stability ranges of the two pure-mode solutions and the mixed-mode solution as the forcing γ is varied. The vertical axis is $R = \sqrt{|B_0|^2 + |B_k|^2}$. The solid (dashed) curves denote stable (unstable) solutions. The thin vertical lines in (a) and (b) highlight the location of the uniform-oscillation boundary, $\gamma = \gamma_{\rm b}$. Note that in (b) the uniform-oscillation boundary lies inside the stable mixed-mode region. Parameters: $\mu = 0.1$, $\nu = 2$, $\alpha = 0.5$, (a) $\beta = 0.4$ and (b) $\beta = 0.55$.

Inserting the expansion (6) into eq. (2), solving the linear equations at order μ, evaluating the solvability condition at order $\mu^{3/2}$ and rescaling, we find the amplitude equations

$$\dot{B}_0 = (\mu - i\vartheta)B_0 - (a_r + ia_i)|B_0|^2 B_0 - (c_r + ic_i)|B_k|^2 B_0\,, \tag{7a}$$

$$\dot{B}_k = (\mu + \rho\vartheta)B_k - r_1|B_k|^2 B_k - r_2|B_0|^2 B_k\,, \tag{7b}$$

where $\vartheta = (\gamma - \gamma_{\rm c})/\alpha$, $a_r = 4$, $a_i = 2(2\rho^2+1)\beta/\alpha\rho$, $c_r = 8\rho\eta$, $c_i = 4[2\alpha\rho(\alpha+1) + (3\rho + \alpha)]\beta/\alpha - 4\eta$, $r_1 = 6\rho\eta(1-\beta/\alpha)$, $r_2 = 8 - 12\beta/\alpha$ and $\eta = \alpha + \rho$.

Equations (7) admit three types of non-trivial solutions [18]:

a pure Hopf mode:

$$B_0 = \sqrt{\mu/4}\, e^{-i\Omega_0 t}, \qquad B_k = 0; \tag{8a}$$

a pure Turing mode:

$$B_0 = 0, \qquad B_k = \sqrt{\alpha[\mu + \rho\vartheta]/[6\rho\eta(\alpha - \beta)]}; \tag{8b}$$

a mixed Hopf-Turing mode:

$$\begin{aligned} B_0 &= \sqrt{[-(3\beta+\alpha)\mu - 4\alpha\rho\vartheta]/[4(9\beta - 5\alpha)]}\, e^{-i\Omega_M t}, \\ B_k &= \sqrt{[(3\beta-\alpha)\mu + \alpha\rho\vartheta]/[2\rho\eta(9\beta - 5\alpha)]}, \end{aligned} \tag{8c}$$

where $\Omega_0 = \vartheta + a_i|B_0|^2$ and $\Omega_M = \vartheta + a_i|B_0|^2 + c_i|B_k|^2$ [19].

A linear stability analysis of the pure Turing solution (using eqs. (7)) gives the stability threshold $\alpha = \beta$; stationary Turing patterns are unstable for $\beta > \alpha$. A linear stability analysis of the mixed-mode solution gives the stability threshold $\beta = 5\alpha/9$: mixed-mode oscillations are unstable for $\beta < 5\alpha/9$. We therefore consider the range $\beta > 5\alpha/9$ which allows for stable mixed-mode oscillations, and distinguish between two cases: Case a) $5\alpha/9 < \beta < \alpha$, and Case b) $\beta > \alpha$.

Figure 3 shows bifurcation diagrams for the amplitude of the Turing, Hopf, and mixed-mode solutions in the two cases. In Case a) (fig. 3(a)), uniform oscillations are stable for forcing amplitudes up to $\gamma = \gamma_{\rm H}$, where

$$\gamma_{\rm H} = \gamma_{\rm c} + \frac{\mu}{\rho}(\alpha - 3\beta). \tag{9}$$

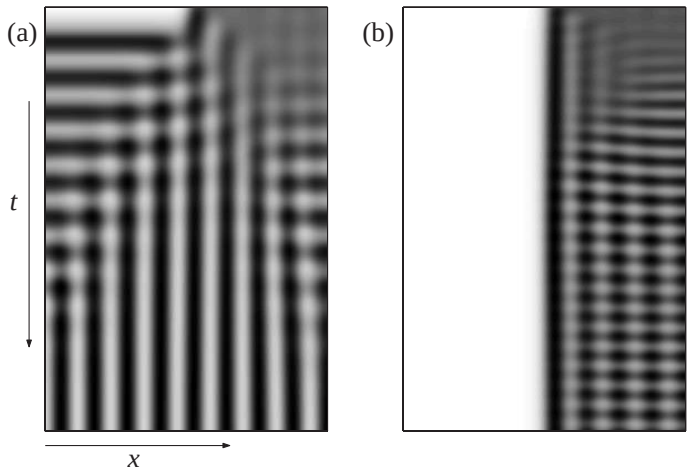

Fig. 4 – Space-time plots of numerical solutions of eq. (2) using Neumann boundary conditions. (a) The development of a pure Turing mode (resonant pattern) outside the 2 : 1 resonance tongue for $\beta < \alpha$ and $\gamma > \gamma_{\rm S}$ (point "R" in fig. 5(a)). The transverse stripes represent unstable Hopf oscillations. (b) Persistent coexistence of a uniform phase state with mixed-mode oscillations inside the 2 : 1 resonance tongue for $\beta > \alpha$ and $\gamma < \gamma_{\rm M}$ (point "N" in fig. 5(b)). In both cases, the initial conditions consist of one of the phase states (3) occupying one half of the x domain and the unstable rest state $A = 0$ occupying the other half. The frames show a grey-scale image of the $\mathrm{Re}\, A$ field. Darker shades denote higher $\mathrm{Re}\, A$ values. Parameters: $\mu = 0.1$, $\nu = 2$, $\alpha = 0.5$, $x = [0, 64]$, (a) $\beta = 0.4$, $\gamma = 1.77$, $t = [0, 100]$, and (b) $\beta = 0.55$, $\gamma = 1.72$, $t = [0, 160]$.

Beyond this threshold and up to $\gamma = \gamma_{\rm S}$, where

$$\gamma_{\rm S} = \gamma_{\rm c} - \frac{\mu}{4\rho}(\alpha + 3\beta), \tag{10}$$

stable mixed-mode oscillations appear. Beyond $\gamma_{\rm S}$ stable Turing solutions prevail to the tongue boundary, $\gamma = \gamma_{\rm b}$, and beyond.

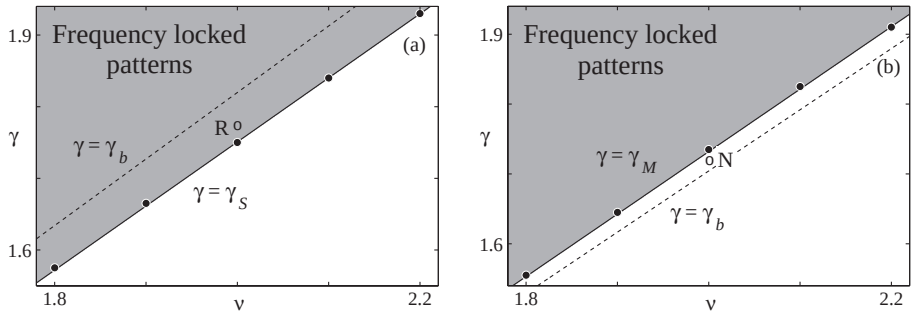

Fig. 5 – The boundaries of resonant patterns as computed from eqs. (10) and (11) (solid lines) *vs.* the boundaries of resonant uniform oscillations (dashed lines). The solid circles indicate the boundaries obtained from direct numerical solution of eq. (2). Shaded areas denote resonant dynamics. In (a) the effect of the Turing mode is to extend the range of resonant dynamics, whereas in (b) the effect is to reduce it. The points "R" ($\gamma = 1.77$, $\nu = 2$) and "N" ($\gamma = 1.72$, $\nu = 2$) correspond to the resonant and non-resonant patterns shown in figs. 4(a) and (b), respectively. Parameters: $\mu = 0.1$, $\alpha = 0.5$, and (a) $\beta = 0.4$ and (b) $\beta = 0.55$.

Case b) (fig. 3(b)), like Case a), involves a transition from pure mode oscillations to mixed-mode oscillations at $\gamma = \gamma_{\rm H}$, but unlike Case a), the stability of the mixed-mode oscillations persists beyond the tongue boundary, $\gamma = \gamma_{\rm b}$. Mixed-mode oscillations destabilize at $\gamma = \gamma_{\rm M}$ (assuming $\nu > \mu(\beta^2 - 1)/(2\beta)$ [13]), where

$$\gamma_{\rm M} = \gamma_{\rm c} - \frac{\mu[(3\beta - 2\alpha)^2 + 3\beta\alpha]}{\rho\,(3\beta + \alpha)}\,. \tag{11}$$

The significance of the results described above for Case a) is that stable *resonant* standing waves, represented by stationary solutions of (7), exist in the range $\gamma_{\rm S} < \gamma < \gamma_{\rm b}$ *outside* the 2 : 1 resonance tongue of uniform oscillations. The stationary solutions form through the Turing instability as demonstrated in a numerical solution of eq. (2) shown in fig. 4(a).

For Case b) in the parameter range $\gamma_{\rm b} < \gamma < \gamma_{\rm M}$, inside the resonant tongue for uniform solutions, the non-resonant mixed-mode oscillations stably coexist with the phase-state solutions of (2). Figure 4(b) shows a numerical solution of eq. (2) with a uniform phase-state in one half of the domain and mixed-mode oscillations in the other half (the phase-state solutions are not captured by the amplitude equations (7) as the ansatz (6) does not contain them). Non-resonant (mixed-mode) oscillations can therefore be realized within the 2 : 1 resonance tongue for uniform solutions.

Above $\gamma_{\rm M}$ the mixed-mode oscillations are unstable and patterns evolve toward a mixture of the two phase states (3) which represent resonant oscillations of the original system.

The new boundaries of resonant oscillations for both cases of the extended system are shown in fig. 5. In fig. 5(a) a point "R" outside the resonance tongue of uniform oscillations (dashed line) gives rise to a *resonant* stripe pattern as shown in fig. 4(a), whereas in fig. 5(b) a point "N" inside the resonance tongue of uniform oscillations gives rise to *non-resonant* mixed-mode oscillations as shown in fig. 4(b).

The parameter ranges considered in this study are limited but sufficient to demonstrate the existence of resonant spatial patterns outside the 2 : 1 resonance tongue, and the existence of non-resonant patterns inside the tongue. Another mechanism (other than mixed-mode oscillations) that leads to non-resonant patterns inside the 2 : 1 resonance tongue is the non-equilibrium Ising-Bloch (NIB) bifurcation [12, 20]. This mechanism is addressed in ref. [17]. The predictions of this study can be tested in experiments on the periodically forced photosensitive Belousov-Zhabotinsky reaction [6].

* * *

We thank ANNA LIN and HARRY SWINNEY for helpful discussions. This research was supported by the US-Israel Binational Science Foundation (grant No. 9800129) and by the Department of Energy under contracts W-7405-ENG-36 and the DOE Office of Science Advanced Computing Research (ASCR) program in Applied Mathematical Sciences. CE acknowledges the support of Fondecyt under grant No. 1020374.

REFERENCES

[1] ARNOL'D V. I., *Geometrical Methods in the Theory of Ordinary Differential Equations* (Springer-Verlag, New York) 1983; JENSEN M. H., BAK P. and BOHR T., *Phys. Rev. A*, **30** (1984) 1960.

[2] We use the term "Turing instability" in the broad sense of a stationary, finite-wave-number instability, rather than a finite-wave-number instability resulting specifically from appropriate values of diffusion coefficients. See CROSS M. C. and HOHENBERG P. C., *Rev. Mod. Phys.*, **65** (1993) 851.

[3] Eiswirth M. and Ertl G., *Phys. Rev. Lett.*, **60** (1988) 1526.
[4] Brown S. E., Mozurkewich G. and Grüner G., *Phys. Rev. Lett.*, **52** (1984) 2277.
[5] Glass L., *Nature*, **410** (2001) 277.
[6] Petrov V., Ouyang Q. and Swinney H. L., *Nature*, **388** (1997) 655.
[7] Bak P., *Phys. Today*, **39** (1986) 38, and references therein.
[8] Coullet P., Frisch T. and Sonnino G., *Phys. Rev. E*, **49** (1994) 2087.
[9] Aranson I. S., Tsimring L. S. and Vinokur V. M., *Phys. Rev. E*, **59** (1999) R1327.
[10] Park H.-K., *Phys. Rev. Lett.*, **86** (2001) 1130.
[11] Gambaudo J. M., *J. Diff. Eq.*, **57** (1985) 172; Elphick C., Iooss G. and Tirapegui E., *Phys. Lett. A*, **120** (1987) 459.
[12] Coullet P., Lega J., Houchmanzadeh B. and Lajzerowicz J., *Phys. Rev. Lett.*, **65** (1990) 1352.
[13] The form of the resonance boundary changes to $\gamma_{\rm b} = \sqrt{\mu^2 + (\mu\beta - 2\nu)^2}/2$ for $\nu < \mu(\beta^2-1)/(2\beta)$ (assuming $\beta > 0$ which is used here). For further details see ref. [15].
[14] Yochelis A. *et al.*, *SIAM J. Appl. Dyn. Sys.*, **1** (2002) 236.
[15] Yochelis A., PhD Thesis, Ben Gurion University (2003).
[16] Battogtokh D. and Browne D., *Phys. Lett. A*, **266** (2000) 359.
[17] Yochelis A., Elphick C., Hagberg A. and Meron E., *Two-phase resonant patterns in forced oscillatory systems: Boundaries, mechanisms and forms*, unpublished (2004).
[18] Keener J. P., *Stud. Appl. Math.*, **55** (1976) 187; Kidachi H., *Prog. Theor. Phys.*, **63** (1980) 1152; De Wit A., Dewel G. and Borckmans P., *Phys. Rev. E*, **48** (1983) R4191; De Wit A., Lima D., Dewel G. and Borckmans P., *Phys. Rev. E*, **54** (1996) 261; Meixner M., Bose S. and Schöll E., *Physica D*, **109** (1997) 128; Meixner M., De Wit A., Bose S. and Schöll E., *Phys. Rev. E*, **55** (1997) 6690; Just W. *et al.*, *Phys. Rev. E*, **64** (2001) 26219.
[19] The solutions (8) are members of continuous families of solutions obtained by multiplying the amplitudes B_0 and B_k by arbitrary constant phase factors of the form $\exp[i\psi]$.
[20] Elphick C., Hagberg A., Meron E. and Malomed B., *Phys. Lett. A*, **59** (1997) 255.